

PAPER



Cite this: *Dalton Trans.*, 2015, **44**, 1456

Dynamic magnetism of an iron(II)-chlorido spin chain and its hexametallic segment†

Lei Qin,^{‡a} Zhong Zhang,^{‡a} Zhiping Zheng,^{a,b} Manfred Speldrich,^c Paul Kögerler,^c Wei Xue,^d Bao-Ying Wang,^d Xiao-Ming Chen^d and Yan-Zhen Zheng^{*a}

An air-stable iron(II) chain compound [Fe(phen)(Cl)₂]_n (**1**, phen = 1,10-phenanthroline) was prepared and exhibits intrachain ferromagnetic interactions as well as competing interchain antiferromagnetic interactions that are mediated by π - π stacking of the phen ligands, resulting in metamagnetic behaviour. The interchain interactions can be altered by changing the external magnetic field, and disparate magnetic dynamics was thus observed from zero to the critical field of 1500 Oe. Zero-field cooled (ZFC) and field-cooled (FC) magnetization and heat capacity measurements indicate that long-range antiferromagnetic ordering occurs at lower fields, and this ordering disappears when the external field is larger than 1500 Oe. The low-frequency ac susceptibility data are consistent with the exponential increase of the temperature-dependent dc data, indicating a Glauber-type dynamics under the field of 1500 Oe. Thus, **1** is considered as a metamagnetic single-chain magnet. For further analysis, a discrete hexametallic segment of the chain, [Fe₆(phen)₆(Cl)₁₂] (**2**), was also isolated and was shown to possess a high-spin ground state and display slow magnetic relaxations like single-molecule magnets. Magnetic analysis using CONDON suggests weak ferromagnetic interactions between the metal centres. The polymeric compound **1** can be viewed as being constructed using the hexametallic unit **2** which is of a low energy barrier, suggesting the significance of intrachain ferromagnetic interactions in enhancing the spin-reversal energy barrier of the short chains.

Received 27th August 2014,
Accepted 12th November 2014

DOI: 10.1039/c4dt02599g

www.rsc.org/dalton

Introduction

There has been continuous interest in developing molecule-based magnetic materials with the possibility of uncovering exotic magnetic phenomena.¹ Many of these interesting magnetic behaviours are attributed to ferromagnetic interactions that can lead to high ground-spin states (S_T) and large magnetic moments. Together with a significant uniaxial magnetic anisotropy (D), superparamagnet-like slow-relaxation and magnetic bistability below the blocking temperature could also be observed. Representatives of such interesting magnetic

systems include single-molecule magnets (SMMs)² and single-chain magnets (SCMs),³ with the latter being usually related to the former, especially from the magnetic dynamics point of view. The energy barrier for spin-reversal of an SMM is expressed as $|D|S_T^2$ (for integer S_T), whilst the latter has an extra barrier (Δ_E) originating from intrachain exchange-coupling.

Clearly, a complete analysis of the intrachain magnetic interactions is critical for establishing magneto-structural correlation in SCMs, which necessitates the isolation of the constitutional spin units of a chain system. A small number of reports of such efforts have appeared in the literature, which are significant not only to our understanding of spin-chain magnetic dynamics, but also to the rational assembly of SCMs. The groups of Clérac and Miyasaka demonstrated the first attempt.⁴ The comprising {Mn₂} dimer of the first heterometallic SCM [Mn₂(saltmen)₂Ni(pao)₂-(py)₂]_n·2n(ClO₄) (saltmen = *N,N'*-(1,1,2,2-tetramethylethylene)-bis(salicylideneimine), pao = pyridine-2-aldoximate and py = pyridine) was isolated and confirmed to be an SMM,⁵ whilst the {Ni-Mn} linkage shows antiferromagnetic interaction.^{6,7} The groups of Julve⁸ and Gao⁹ also successfully isolated their own SCM building units and clarified the magnetic correlation between the oligomer and the chain. These pioneering studies demon-

^aCenter for Applied Chemical Research, Frontier Institute of Chemistry, Frontier Institute of Science and Technology, and State Key Laboratory for Mechanical Behavior of Materials, Xi'an Jiaotong University, Xi'an 710054, China.

E-mail: zheng.yanzhen@mail.xjtu.edu.cn

^bDepartment of Chemistry, The University of Arizona, Tucson, Arizona 85721, USA

^cInstitute of Inorganic Chemistry, RWTH Aachen University, D-52074 Aachen, Germany

^dMOE Key Laboratory of Bioinorganic and Synthetic Chemistry, School of Chemistry & Chemical Engineering, Sun Yat-Sen University, Guangzhou 510275, China

†Electronic supplementary information (ESI) available. CCDC 959874. For ESI and crystallographic data in CIF or other electronic format see DOI: 10.1039/c4dt02599g

‡These authors contributed equally to this work.

strated the importance of isolating constitutional spin units for an in-depth understanding of spin-chain magnetic dynamics and further paved the way for the rational assembly of prototype SCMs.¹⁰

For Ising systems, the correlation length (ξ) increases exponentially. As such, the linear regime of the natural logarithm of the χT product then directly measures the wall energy ($\ln(\chi T) = \ln C + \ln(\Delta_g/k_B T)$, where C is the Curie constant). Because SMMs have well-isolated ground-spin states, J_1 is usually less comparable to the intramolecular magnetic couplings. As such, SCMs made of a string of SMMs are often the prototypes.^{3,11}

In other cases where SCMs are made of individual metal sites, the differences between the intra- and inter-molecular magnetic interactions are removed. In order to obtain prototype SCMs in such systems, metal ions with large magnetic anisotropy are critical. Thus, most of the single-spin SCMs are made of octahedral cobalt(II) ions, including the first reported SCM by the group of Gatteschi,¹² the first homo-spin SCM by the group of Gao¹³ and the first canted-antiferromagnetic SCM by the group of Dunbar.¹⁴ Other sources of anisotropic metal ions such as dysprosium(III)¹⁵ and iron(II)¹⁶ were also widely employed.

In the past few years, our group has developed a *network approach*¹⁷ to polymerise spin-chains into higher-dimensional coordination networks. We first used the *trans*-1,2-cyclohexane-dicarboxylate to incorporate homo five-coordinate Co(II) ions into a 2D laminated network.¹⁸ The carboxylate-bridged Co(II) chain shows overall ferromagnetic interaction, so that prototype SCM behaviour was achieved. Later, we expanded this method to ligands analogous to 1,2-cyclohexane-dicarboxylate, such as cyclohex-1-ene-1,2-dicarboxylate and *trans*-4-methylcyclohexane-1,2-dicarboxylate,¹⁹ and other related ligands, such as *trans*-cyclohexane-1,4-dicarboxylate,²⁰ 4-carboxylphenoxyacetate,²¹ 2-(pyridin-3-yloxy)acetate²² and benzophenone-2,4'-dicarboxylate.²³ All these carboxylates can incorporate metal-(hydroxy)carboxylate chains into higher dimensional coordination networks, thus offering a unique opportunity for studying the interchain magnetic interactions on spin dynamics.²⁴ However, the drawbacks of such polymeric systems are also obvious; especially the poor solubility in a common solvent prevents the isolation of constitutional spin units for further analysis.

As an ongoing study of magnetic chains,²⁵ herein we synthesise an interesting spin-2 chain $[\text{Fe}(\text{phen})(\text{Cl})_2]_n$ (**1**, phen = 1,10-phenanthroline) featuring individual Fe(II) centres doubly bridged by chlorido groups with ancillary phen ligands by the reported method.^{25,26} Synthesis using a different solvent under otherwise identical reaction conditions led to the production of a linear hexametallic complex $[\text{Fe}_6(\text{phen})_6(\text{Cl})_{12}]$ (**2**) which can be viewed as a fragment of **1** with the propagation of the polymeric chain being arrested by two additional chlorido groups, one on each terminal of the linear complex. Powder X-ray diffraction experiments confirm the purity of both compounds (Fig. S1†). The combination of **1** and **2** is ideal for comparative magnetic studies for the delineation of the relation-

ship between a polymeric magnetic chain and its building units in terms of the contribution of intrachain interactions to the overall magnetic dynamics of the polymeric structure.

Results and discussion

Syntheses

Compounds **1** and **2** were prepared under otherwise identical solvothermal conditions except for the different solvent used, with **1** obtained from acetylacetone and **2** from ethanol. It is clear that the nature of the solvent used is critical to the identity of the products, which has been observed also in our previous work. Equally important for the termination of the propagation of the polymer chain is the flexible coordination of the metal centres; only those exhibiting flexible coordination numbers can be terminated to achieve the oligomeric fragment of the polymeric chains.

Structural analyses

Both compounds were characterized by elemental analyses and structurally determined by single crystal X-ray diffraction studies. Compound **1** crystallizes in the monoclinic space group $C2/c$ (Fig. 1). Its molecular structure was reported previously,²⁶ which features an infinite $[\text{Fe}^{\text{II}}-(\mu\text{-Cl})_2-\text{Fe}^{\text{II}}-(\mu\text{-Cl})_2]_n$ chain sheathed by peripheral phen ligands on both sides of the chain. The Fe(II) ions are disposed in a zigzag fashion (Fig. 1a) with a separation of 3.76 Å between neighbouring Fe(II) centres and an $\text{Fe}\cdots\text{Fe}\cdots\text{Fe}$ angle of 133.9°. The extended chain structure can be viewed as constructed using repetitive diamond-shaped units of $\{\text{Fe}(\mu\text{-Cl})_2\text{Fe}\}$ where the Fe(II) centre is also coordinated with a phen ligand. Thus, each Fe(II) is situated in a

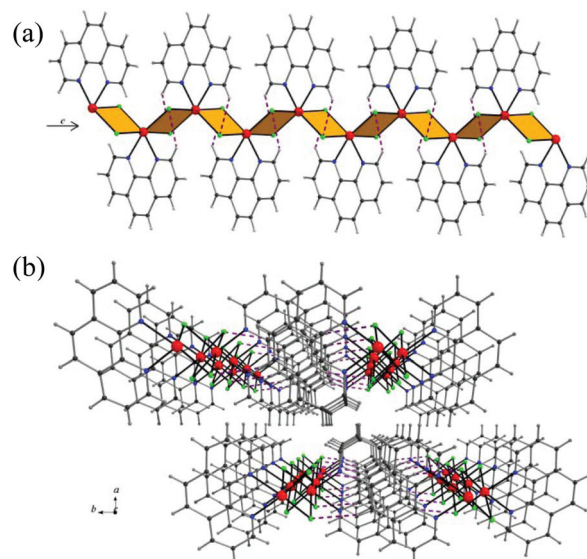


Fig. 1 Single-stranded chain structure (a) and the crystal packing (b) of **1**. Purple dotted lines indicate C–H \cdots Cl hydrogen bonds. Colour codes (the same in the following figure): Fe, red; Cl, green; C, dark gray; H, gray.

slightly distorted octahedral coordination environment. The neighbouring $\{\text{Fe}(\mu\text{-Cl})_2\text{Fe}\}$ units are nearly mutually perpendicular, forming a dihedral angle of 81.4° . The Fe–Cl bond lengths range from 2.415(3) to 2.639(3) Å while the Fe–N distance is 2.182(9) Å. The phen ligands are parallel to each other and perpendicular to the direction of the chain extension. The planar ligands are also engaged in face-to-face π – π interactions between adjacent chains²⁷ with a centroid-to-centroid separation averaged at 3.51 Å. The interchain interactions are further reinforced by pair-wise hydrogen bonds involving two phen C–H bonds and the chlorido groups. The C–H...Cl angles of 147.6° – 167.9° are comparable to the analogous hydrogen bonds in the previously reported $\{\text{Mn}_4\}$ dimers²⁸ and a $\{\text{Co}_4\}$ chain.^{25a}

Compound **2** crystallizes in the triclinic space group $P\bar{1}$. The linear arrangement of the six Fe(II) centres is identical to what is present in the polymeric structure of **1**, but the terminal Fe(II) ions are each capped by a chlorido group, thus terminating the propagation of the chain and hence the discrete oligomeric structure (Fig. 2). While each of the four inside Fe(II) centres is hexacoordinate, just as in the case of **1**, the terminal Fe(II) ions are each pentacoordinate, featuring the chelation of a phen ligand, and two bridging and one terminal chlorido groups. The metal centres in **2** are also arranged in a zigzag fashion, but with smaller Fe...Fe angles, ranging from 129.43° to 132.35° . The Fe...Fe separations are also uneven, increasing gradually from 3.55, 3.69 to 3.70 Å moving from the periphery toward the center of the complex. Similar to **1** the crystal packing of **2** is also dominated by interchain

π – π stacking interactions of the phen ligands and the aforementioned C–H...Cl hydrogen bonds.

Magnetic properties of **1**

Metamagnetism. DC magnetic measurements of **1** reveal overall intrachain ferromagnetic interactions and metamagnetism at low temperatures (Fig. 3a). At room temperature (300 K), the χT value is $3.70 \text{ cm}^3 \text{ mol}^{-1} \text{ K}$, which is larger than the expected spin-only value ($3.00 \text{ cm}^3 \text{ mol}^{-1} \text{ K}$) for one uncoupled Fe(II) ion, but nevertheless consistent with other octahedral Fe(II)-based compounds.²⁹ Upon cooling, the χT value increases gradually until the temperature goes down to 50 K. In this region, the susceptibility data are well fitted by the Curie–Weiss law, producing a C -value of $3.61 \text{ cm}^3 \text{ mol}^{-1} \text{ K}$ and a θ value of 10.2 K. The moderate positive θ value may indicate ferromagnetic coupling between the Fe(II) ions.³⁰ This conclusion is further supported by the χT plot below 50 K; a rapid increase up to a maximum of $9.65 \text{ cm}^3 \text{ mol}^{-1} \text{ K}$ at 6.0 K is followed by a sharp decrease afterwards. The presence of the maximum in the χT plot may indicate a long-range magnetic ordering in **1**. The susceptibility data from 300 to 10 K can be well simulated by the Fisher model, eqn (1),³¹

$$\chi_{\text{chain}} = \frac{N(M\beta)^2 (1-u)}{3k_B T (1+u)} \quad (1)$$

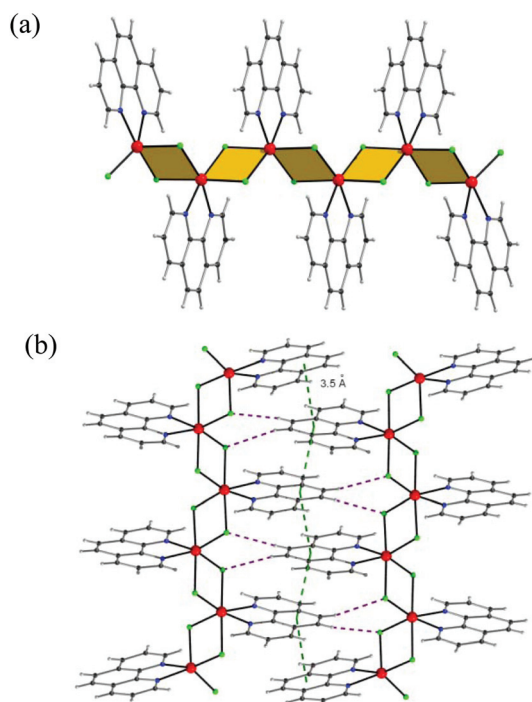


Fig. 2 The molecular structure (a) and the crystal packing (b) of **2**. Green dotted lines indicate the π – π interactions between the phen ligands.

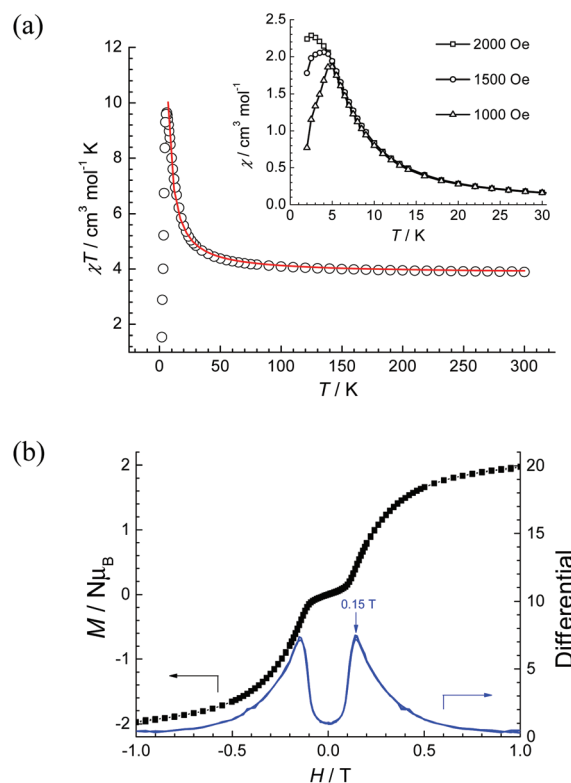


Fig. 3 (a): Temperature dependence of χT and χ_m (inset) of **1**, referred to one Fe(II) ion, at the indicated applied fields. Red solid line: fitting result using eqn (1). (b): Isothermal magnetization and its derivative of **1** measured at 2 K.

where $M = g[S(S + 1)]^{1/2}$ and $u = \coth(J/k_B T) - k_B T/J$. In order to fit experimental data, the exchange energy J must be scaled by following the usual procedure: $J \rightarrow JS(S + 1)$. The best fitting gives $J = 1.25(2)$ K and $g = 2.262(8)$. The positive J value indicates weak ferromagnetic interactions in the chlorido-bridged Fe(II) chain, which has been reported also in the literature.³²

The field-dependent metamagnetic behaviour is evidenced from the χ vs. T plots (insets, Fig. 3a). Below 1500 Oe there is an obvious cusp in the χ vs. T plot, indicating the antiferromagnetic phase. The cusp disappears above 1500 Oe and is saturated at 2000 Oe. This means that the interchain magnetic interactions are antiferromagnetic in nature and can be overcome by altering the magnetic field.

To assess this critical field, isothermal magnetization of **1** between ± 1 T was measured at 2 K (Fig. 3b). The absence of the hysteresis effect coincides with the antiferromagnetic phase, and the expected “transit” is observed in the origin region. From the derivative of the magnetisation plot, the critical field H_c can be determined as 1.5 kOe. The weak interchain magnetic interaction³³ thus can be estimated from eqn (2),³⁴

$$g\mu_B H_c S = 2|zJ'|S^2 \quad (2)$$

The obtained value of $|zJ'|$ is 0.06 K. Assuming that $z = 2$, $|J'|$ is valued at 0.03 K. After obtaining the $|J'|$ value, we can use it to estimate the T_c value using eqn (3),³⁵

$$k_B T_c = 4S(S + 1)|JJ'|^{1/2} \quad (3)$$

The resulting $T_c = 6.7$ K is in excellent agreement with the maximum in the χT plot at 6.0 K. The occurrence of long-range magnetic ordering behaviour would be attributed to the extensive π - π stacking and C-H \cdots Cl hydrogen-bonding interactions.

Evidence of long-range antiferromagnetic ordering. In order to understand the nature of the possible long range ordering, zero field cooling and field cooling magnetic susceptibility plots from 2 to 30 K were obtained under 100, 1500 and 2000 Oe dc fields, respectively (Fig. 4). Upon 100 Oe, the χ plots for both ZFC and FC merge clearly, both with an obvious sharp peak at around 5 K, which may prove the long range magnetic ordering transition.³⁶ When the external magnetic field is larger than 1500 Oe the interchain antiferromagnetic interaction starts to be overcome by the external magnetic field

and the spin thus reorients, resulting in the disappearance of the magnetic ordering transition. This is in accordance to the linear increase of $M(H)$ below 1500 Oe (Fig. 3b). The χT vs. T^{-1} plots under different fields are presented in Fig. S2,[†] confirming that the paramagnetic/antiferromagnetic phase transition temperature is around 5 K.^{37a} Further evidence was provided by the specific heat capacity measurements under different fields (Fig. 5). The data under zero field affords an explicit λ -type anomaly at about 4.8 K and this anomaly vanishes as the field increases, further confirming the existence of a 3D long range order state arising from the interchain couplings.^{37,38}

Coexistence of SCM dynamics. To further investigate the magnetic behaviour of **1**, the temperature dependence of the ac susceptibility was measured in zero, 1000 and 1500 Oe applied dc fields. As shown in Fig. 6a, in zero field, the in-phase (χ') component of the ac susceptibility shows a cusp at 5 K, further confirming the long-range antiferromagnetic ordering. However, below 2.5 K a frequency-dependent shoulder of $\chi'(T)$ and the corresponding out-of-phase (χ'') component of the ac susceptibility were observed. Although this relaxation behaviour is not prominent it indicates the presence of fluctuation in this ordering phase, which is presumably caused by the competing SCM dynamics (see below). This phenomenon of coexistence of ordering phase and SCM dynamics has been recently observed theoretically and experi-

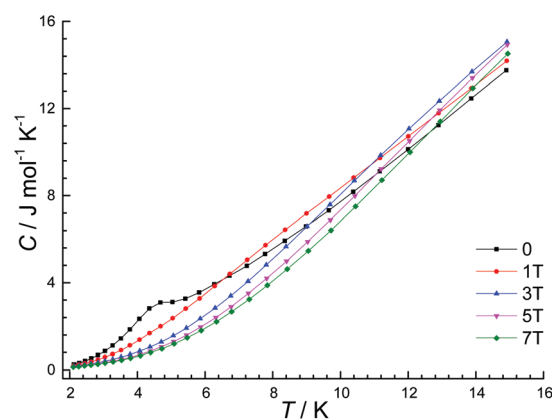


Fig. 5 Molar specific heat measured under the indicated dc fields for **1**.

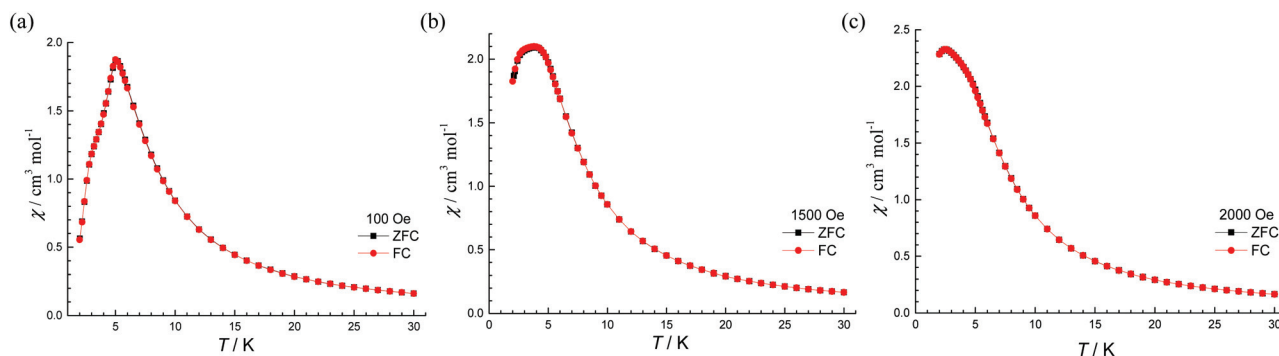


Fig. 4 The ZFC-FC magnetization measured under dc fields of 100 Oe (a), 1500 Oe (b) and 2000 Oe (c) from 2 to 30 K for **1**.

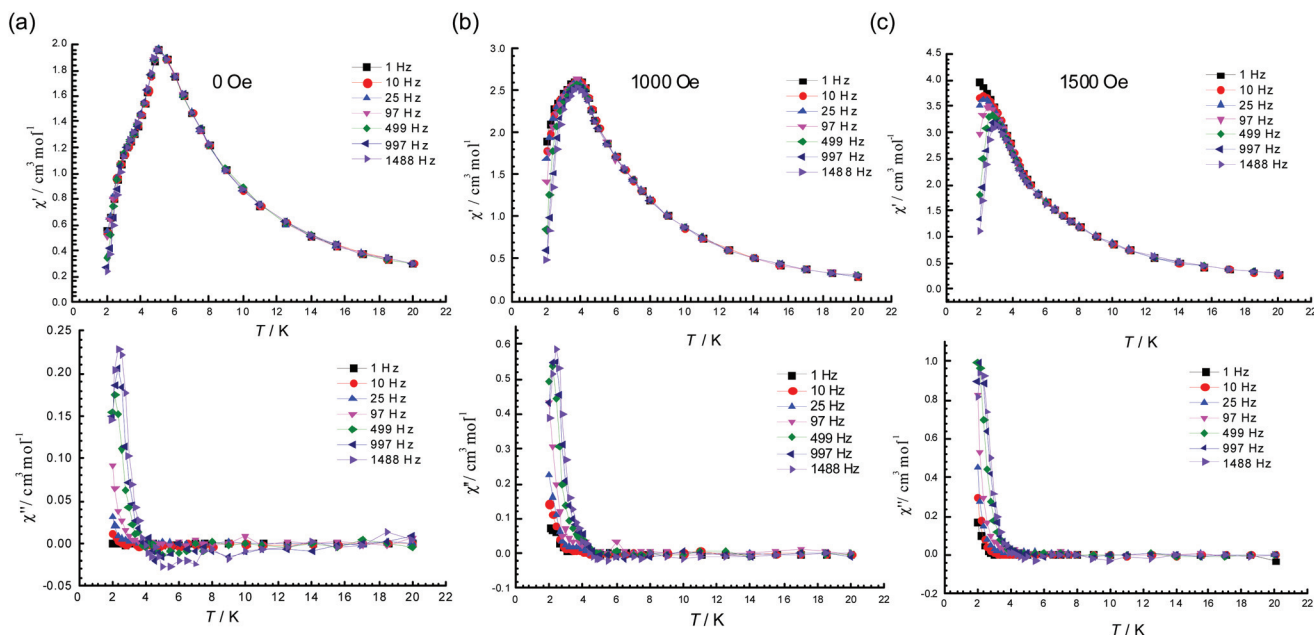


Fig. 6 The temperature dependence of the real, χ' , upper plot, and the imaginary, χ'' , lower plot, components of the ac susceptibility of **1** measured in an applied dc field of 0 Oe (a), 1000 Oe (b) and 1500 Oe (c).

mentally, especially from the groups of Sibille, Coulon, Clérac and Miyasaka.^{37,38} Related dynamic magnetic behaviour in ordered “very hard” 1D materials has also been reported by the group of Ishida,³⁹ which was later postulated to be a result of slow-relaxation by Sessoli.⁴⁰

Under 1000 Oe dc field, both $\chi'(T)$ and $\chi''(T)$ exhibit stronger frequency-dependent behaviour; the maximum value of $\chi'(T)$ increases by a factor of ca. 2.5 as compared to the zero-field value, see Fig. 6b. This tendency has been strengthened in the dc field of 1500 Oe. As shown in Fig. 6c, the 1 Hz of $\chi'(T)$ has no downturn down to 2 K and other frequencies of $\chi'(T)$ go up progressively; the maximum value of $\chi''(T)$ increases by a factor of ca. 4 as compared to the zero-field value; and the maximum in $\chi'(T)$ is only three times larger in magnitude than that for $\chi''(T)$, indicating a Lorenz relation. If T_p is the temperature of the maximum in χ' and f is the frequency of the ac field, the frequency dependence of T_p is given by $\phi = (\Delta T_p / T_p) / \Delta(\log f)$.⁴¹ Under the dc field of 1500 Oe, ϕ of **1** is slightly greater than 0.10, a value that indicates a superparamagnetic-like behavior rather than a spin-glass behavior.⁴²

To further examine whether the dynamic magnetic behaviour of **1** obeys the Glauber model, where χ diverges exponentially as

$$\chi T = C_{\text{eff}} \exp(\Delta\xi/k_B T) \quad (4)$$

The logarithm of χT vs. $1/T$ has been plotted (Fig. 7) and the linear regime fitting from 10 to 80 K gives $\Delta\xi/k_B = 7.9(1)$ K. As long as $\Delta\xi/k_B = 4J_{\text{eff}}/k_B$, the derived J_{eff} is in good agreement with the J' value obtained from the Heisenberg model. Furthermore, the $\ln(\chi T)$ vs. T^{-1} saturates at the lowest temperatures, i.e., below ca. 5 K, because of finite size effects.⁴³ However, for an infinite chain with substantial anisotropy, the gap acti-

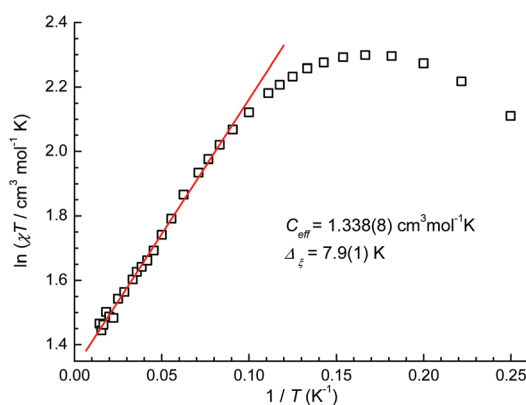


Fig. 7 The logarithm of χT vs. $1/T$ for **1**. The dc susceptibility was obtained in an applied field of 1500 Oe. The red line is the result of a linear fit between 10 and 80 K.

vation energy is given by $\Delta_\tau = 2\Delta_\xi + \Delta_A$, where Δ_A is the activation energy resulting from the single-ion anisotropy, i.e., $\Delta_A = |D|S^2$, an energy which, in turn, depends on the single ion anisotropy constant, D , of the iron(II) ion. As long as Δ_τ in **1** under field excitation is obviously not high, the contribution from the Δ_A term is small or diminished by the fast quantum tunnelling effect.

Magnetic properties of **2**

Temperature-dependent dc susceptibility data of **2** have been measured with a polycrystalline sample (Fig. 8). At room temperature, the χT product is higher than the spin-only value of six uncoupled Fe(II) metal centres (calc. $18 \text{ cm}^3 \text{ mol}^{-1} \text{ K}$ for $s = 2$ and $g = 2$), indicating a significant orbital contribution to the magnetic moment. Upon cooling, the χT product increases

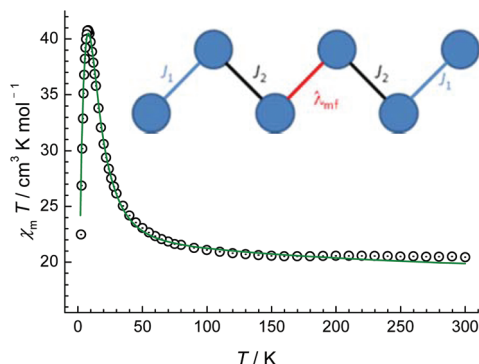


Fig. 8 The χT vs. T data measured under 1000 Oe for **2**. Solid line: the best fit from eqn (5). Insert: the magnetic coupling model used for fitting.

gradually and then sharply before and below 50 K, respectively. The ascending of the χT product implies a high-spin ground state of the molecule, which ferromagnetic interactions between the metal centres may account for.

The imaginary part of the ac susceptibility data under zero dc field shows frequency-dependent behaviour for **2** (Fig. 9), indicating the similar dynamic magnetism. According to the theorem of SMMs,² high-spin magnetic molecules with proper axial magnetic anisotropy are promising to be SMMs, which is consistent with the case of **2**. As high-spin iron(II) in a pseudooctahedral coordination environment has substantial magnetic anisotropy (see below) we believe that the zero-field slow magnetic relaxation in **2** has a single-molecule origin. Owing

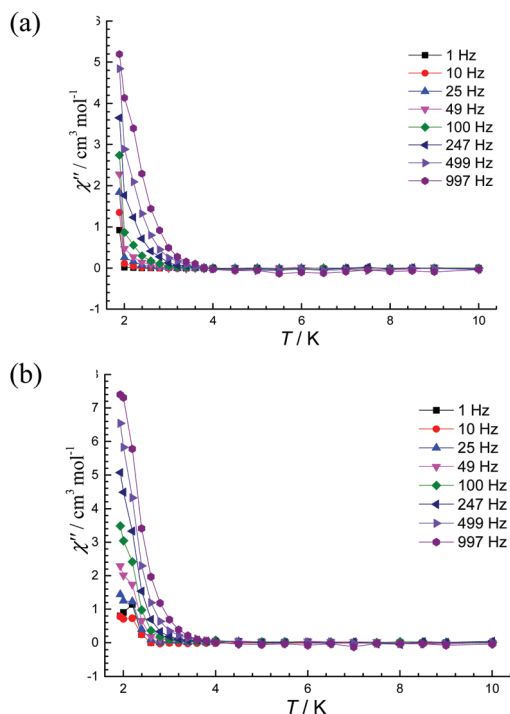


Fig. 9 The χ'' vs. T plot for **2** at indicated frequencies under 0 (a) and 1000 Oe (b).

to the experimental limit we cannot extract reliable energy barriers for both compounds simply from the ac susceptibility data. But the spin-reversal energy barrier of **2** is obviously lower than that of **1** as we can see that all the frequencies show no saturation down to 2 K. Even with the lift of external dc field of 1000 Oe, the quantum tunnelling effects that cost the spin reversal energy barrier cannot be well reduced. This is good indication that the presence of SCM behaviour in **1** does not relate to the lifted SMM behaviour of **2**, further confirming the metamagnetic nature of **1**.

The dc magnetic data were analyzed using the program CONDON 2.0⁴⁴ with a complete basis set (full d manifolds, *i.e.*, 210 functions for Fe^{2+}) as a function of the applied field $B = 0.1$ T, which is necessary to yield reliable information on the magnetic dipole orientation with respect to the local symmetry elements. CONDON takes into account the following single-ion effects: the ligand-field effect (H_{lf}), interelectronic repulsion (H_{ee}), spin-orbit coupling (H_{so}), and the applied field (H_{mag}). Generally, for a magnetically isolated $3d^N$ metal ion in a ligand-field (lf) environment in an external magnetic field B , the Hamiltonian of the metal ion is

$$H = H_{\text{ee}} + H_{\text{lf}} + H_{\text{so}} + H_{\text{mag}} \quad (5)$$

The data set of **2** in the temperature range 2–300 K was fitted to the above-stated Hamiltonian using the ligand-field effect, spin-orbit coupling, and exchange coupling. The values for the spin-orbit coupling parameter ($\zeta = 410 \text{ cm}^{-1}$) and Racah parameters ($B = 783 \text{ cm}^{-1}$, $C = 3687 \text{ cm}^{-1}$) were chosen on the basis of the optical spectra.⁴⁵ Approximating the ligand fields of both the five and six coordinated $\text{Fe}(\text{II})$ centres are axially elongated (peripheral/central $\text{Fe}-\text{Cl}_{\text{ax}}$: 2.6/2.4 Å, $\text{Fe}-\text{Cl}_{\text{eq}}$: 2.4/2.3 Å, $\text{Fe}-\text{N}_{\text{eq}}$: 2.1/2.2 Å), and thus the influence of the tetragonal ligand field with reference to the rotation axis for the angular part of the wave function is described by the following Hamiltonian:

$$H_{\text{lf}}^{\text{tet}} = B_0^2 \sum_{i=1}^5 C_0^2(i) + B_0^4 \sum_{i=1}^5 C_0^4(i) + B_4^4 \sum_{i=1}^5 (C_4^4(i) + C_{-4}^4(i)) \quad (6)$$

Note that the number of independent ligand field parameters is limited by the symmetry-determined ratios B_q^k/B_0^k . Based on the inversion symmetry of **2** we describe the hexanuclear chain as a dimer of trinuclear chains. For this model the exchange coupling is grouped into coupling within the central (λ_{mf}) and the two (J_1 and J_2) $\text{Fe} \cdots \text{Fe}$ pairs (inset of Fig. 6). The exchange interactions within the trinuclear chains are considered in the Heisenberg model,

$$H_{\text{ex}} = -2[J_1(S_1S_2) + J_2(S_2S_3)] \quad (7)$$

The exchange interactions between the chains are described by the molecular field approximation

$$\chi_{\text{m}}^{-1} = \chi'_{\text{m}}(B, C, \zeta, B_q^k, J_{\text{ex}}) - \lambda_{\text{mf}} \quad (8)$$

where χ'_{m} represents the single-centre susceptibility and λ_{mf} the molecular field parameter.

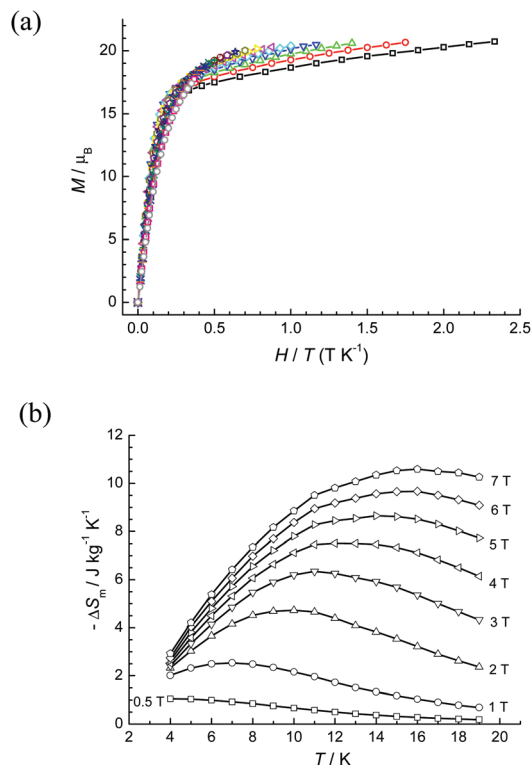


Fig. 10 Plots of M vs. H/T (a) and $-\Delta S_m$ vs. T (b) for **2**.

Standard literature values were chosen as initial values for the real ligand field parameters B_q^k (Wybourne notation).^{46,47} Refining the values B_q^k and J_1, J_2 and λ_{mf} by a least-squares fit adequately reproduces the experimental data (SQ = 1.1%) and yields $B_0^2 = 21\,400\text{ cm}^{-1}$, $B_0^4 = 39\,300\text{ cm}^{-1}$, $B_4^4 = 14\,500\text{ cm}^{-1}$, as well as $J_1 = 1.2\text{ cm}^{-1}$, $J_2 = 1.05\text{ cm}^{-1}$ and $\lambda_{mf} = -0.545 \times 10^4\text{ mol m}^{-3}$. Note that the signs of the refined B_q^k values agree with point-charge electrostatic model results. This fitting result confirms ferromagnetic interactions between the iron(II) centres, which is consistent with the modelling result of **1**.

Plotting the magnetization against the product of H/T shows non-superposition at higher fields (Fig. 10a), which indicates substantial magnetic anisotropy of the complex. Furthermore, the entropy changes ($-\Delta S_m$) calculated from these isothermal magnetization plots show temperature-dependent maximum-shift behaviour (Fig. 10b), that is, shifting to higher temperatures at higher fields. This is also a sign of magnetic anisotropy.⁴⁸

Conclusions

To summarise, we have successfully isolated two iron(II)-chain structures with similar $[\text{Fe}^{\text{II}}-(\mu\text{-Cl})_2]_n$ repeating units. The infinite chain (compound **1**) shows interesting metamagnet-like SCM behaviour due to the combined action of intrachain ferromagnetic interaction and interchain weak magnetic couplings. The finite hexamer (compound **2**) can be viewed as a segment of the infinite chain. The intrachain ferromagnetic

interactions are retained in **2** and thus, **2** shows high-ground spin-state and slow-magnetic relaxation behaviour at lower temperatures. The latter is an indication of a lower energy barrier compared to **1**, which also reflects the importance of intrachain magnetic interactions in enhancing the Glauber activation energy of the Ising-type spin chains. As such, compounds **1** and **2** can be labelled as $\text{M}^{3-1}\text{U}^1\text{S}^1$ and $\text{M}^0\text{U}^0\text{S}^0$, respectively, according to their dimensional correlations between the structure and magnetism.¹⁷

Experimental section

Syntheses

For 1: The solid of $\text{FeCl}_2 \cdot 4\text{H}_2\text{O}$ (0.099 g, 0.5 mmol) was stirred in acetylacetone (20 mL) and then 1,10-phen (0.099 g, 0.5 mmol) was added. After stirring for 20 h at room temperature, the slurry was sealed in a 50 mL Teflon-lined autoclave and heated to 150 °C for 48 h. After cooling to room temperature, red sheet crystals of **1** suitable for single crystal X-ray diffraction were obtained (yield 0.31 g, 20% based on Fe). Elemental analysis (%), calcd: C, 46.95; H, 2.63, N 9.13; found: C, 47.20; H, 2.34; N, 9.25%. IR data for **1** (KBr pellet, cm^{-1}): 3051w, 1622w, 1581m, 1514m, 1421s, 1143s, 1104m, 860s, 783w, 724s, 622w.

For 2: A mixture of $\text{FeCl}_2 \cdot 4\text{H}_2\text{O}$ (0.408 g, 2 mmol), 1,10-phen (0.369 g, 2 mmol) and ethanol (15 mL) was stirred for 10 min in the air in a beaker. The slurry was then sealed in a 20 mL PTFE-lined autoclave and heated to 150 °C. After maintaining at this temperature for 72 h, the autoclave was cooled to room temperature. Red block crystals of **1** suitable for single crystal X-ray diffraction were obtained (yield 0.53 g, 87% based on Fe). Elemental analysis (%), calcd: C, 46.95; H, 2.63, N 9.13; found: C, 46.41; H, 2.32; N, 8.65. IR data for **2** (KBr pellet, cm^{-1}): 3050w, 1622w, 1581m, 1514m, 1421s, 1143s, 1104m, 860s, 783w, 723s, 622w.

Physical measurements

Elemental analyses (C, H and N) were carried out on a Vario EL III elemental analyzer. Magnetic measurements were performed on powder samples by SQUID magnetometry (Quantum Design MPMS-XL). Diamagnetic corrections were calculated from Pascal constants and the holder backgrounds were also corrected. Specific heat experiments of **1** were conducted, from 15 K down to 2 K, on a pressed pellet sample using a Quantum Design PPMS.

Crystallography

Crystal data. For **1**, the unit cell parameters are consistent with the reported data,²⁶ which can be found in CCDC number 625095 or CSD ref POCNEB. For **2**, $\text{C}_{72}\text{H}_{48}\text{Cl}_{12}\text{Fe}_6\text{N}_{12}$, $M = 1841.72$, triclinic, space group $P\bar{1}$, $T = 293(2)\text{ K}$, $a = 10.0016(11)$, $b = 10.2378(11)$, $c = 19.241(2)\text{ Å}$, $\alpha = 80.0380(10)^\circ$, $\beta = 84.4460(10)^\circ$, $\gamma = 61.9170(10)^\circ$, $V = 1711.7(3)\text{ Å}^3$, $Z = 1$, $\rho = 1.787\text{ g cm}^{-3}$, total data 39 581, unique data 7921 ($R_{\text{int}} = 0.0183$), $\mu = 1.762\text{ mm}^{-1}$, 460 parameters, $R_1 = 0.0354$ for

$I \geq 2\sigma(I)$ and $wR_2 = 0.0882$ for all data. The crystal data of **2** were recorded on a Bruker SMART CCD diffractometer with Mo-K α radiation ($\lambda = 0.71073$ Å). The structure was solved by direct methods and refined on F^2 using SHELXTL (Table S1†). Selected coordination bonds and angles are listed in Table S2.† CCDC number 959874 contains the presented crystallographic data.

Acknowledgements

This work was supported by grant nos. 21201137, 2012CB619401, 21473129 and IRT13034, Fundamental Research Funds for the Central University, the “National 1000 Young Talents” program (to YZZ) and the 985 platform for “1000-Plan Global Recruitment” program (to ZZP).

Notes and references

- For recent reviews, see a themed issue: *Molecule-Based Magnets*, ed. J. S. Miller and D. Gatteschi, in *Chem. Soc. Rev.*, 2011, **40**, 3053–3368.
- R. Sessoli, D. Gatteschi and J. Villain, *Molecular Nanomagnets*, Oxford University Press, Oxford, UK, 2006.
- C. Coulon, H. Miyasaka and R. Clérac, *Struct. Bonding*, Springer, Berlin, 2006, **122**, 163.
- (a) R. Clérac, H. Miyasaka, M. Yamashita and C. Coulon, *J. Am. Chem. Soc.*, 2002, **124**, 12837; (b) H. Miyasaka, R. Clérac, K. Mizushima, K.-i. Sugiura, M. Yamashita, W. Wernsdorfer and C. Coulon, *Inorg. Chem.*, 2003, **42**, 8203.
- H. Miyasaka, R. Clérac, W. Wernsdorfer, L. Lecren, C. Bonhomme, K.-i. Sugiura and M. Yamashita, *Angew. Chem., Int. Ed.*, 2004, **43**, 2801.
- H. Miyasaka, T. Nezu, K. Sugimoto, K.-i. Sugiura, M. Yamashita and R. Clérac, *Inorg. Chem.*, 2004, **43**, 5486.
- (a) H. Miyasaka, K. Nakata, K. Sugiura, M. Yamashita and R. Clérac, *Angew. Chem., Int. Ed.*, 2004, **43**, 707; (b) L. Lecren, O. Roubeau, C. Coulon, Y.-G. Li, X. F. Le Goff, W. Wernsdorfer, H. Miyasaka and R. Clérac, *J. Am. Chem. Soc.*, 2005, **127**, 17353; (c) H. Hiraga, H. Miyasaka, K. Nakata, T. Kajiwarra, S. Takaishi, Y. Oshima, H. Nojiri and M. Yamashita, *Inorg. Chem.*, 2007, **46**, 9661.
- (a) H.-B. Xu, B.-W. Wang, F. Pan, R. Lescouëzec, J. Vaissermann, C. Ruiz-Pérez, F. Lloret, R. Carrasco, M. Julve, M. Verdaguer, Y. Draomzee, D. Gatteschi and W. Wernsdorfer, *Angew. Chem., Int. Ed.*, 2003, **42**, 1483; (b) E. Pardo, R. Ruiz-García, F. Lloret, J. Faus, M. Julve, Y. Journaux, F. Delgado and C. Ruiz-Pérez, *Adv. Mater.*, 2004, **16**, 1597; (c) R. Lescouëzec, M. Toma, J. Vaissermann, M. Verdaguer, F. S. Delgado, C. Ruiz-Pérez, F. Lloret and M. Julve, *Coord. Chem. Rev.*, 2005, **249**, 2691; (d) L. M. Toma, R. Lescouëzec, J. Pasán, C. Ruiz-Pérez, J. Vaissermann, J. Cano, R. Carrasco, W. Wernsdorfer, F. Lloret and M. Julve, *J. Am. Chem. Soc.*, 2006, **128**, 4842.
- (a) Z.-M. Wang and S. Gao, *Angew. Chem., Int. Ed.*, 2007, **46**, 7388; (b) X.-Y. Wang, Z.-M. Wang and S. Gao, *Chem. Commun.*, 2008, 281; (c) H.-L. Sun, Z.-M. Wang and S. Gao, *Coord. Chem. Rev.*, 2010, **254**, 1081.
- (a) R. J. Glauber, *J. Math. Phys.*, 1963, **4**, 294; (b) R. Georges, J. J. Borrás-Almenar, E. Coronado, J. Curély and M. Drillon, *One-dimensional Magnetism: An Overview of the Models in Magnetism: Molecules to Materials*, ed. J. S. Miller and M. Drillon, Wiley, Germany, 2001, vol. I, pp. 1–47; (c) H.-J. Mikeska and A. K. Kolezhuk, *One-Dimensional Magnetism in Quantum Magnetism*, ed. U. Schollwöck, J. Richter, D. J. J. Farnell and R. F. Bishop, Springer, Berlin, 2004, pp. 1–83.
- (a) H. Miyasaka, K. Nakata, L. Lollita, C. Coulon, Y. Nakazawa, T. Fujisaki, K.-i. Sugiura, M. Yamashita and R. Clérac, *J. Am. Chem. Soc.*, 2006, **128**, 3770; (b) Y.-L. Bai, J. Tao, W. Wernsdorfer, O. Sato, R.-B. Huang and L.-S. Zheng, *J. Am. Chem. Soc.*, 2006, **128**, 16428; (c) I.-R. Jeon, R. Ababei, L. Lecren, Y.-G. Li, W. Wernsdorfer, O. Roubeau, C. Mathonière and R. Clérac, *Dalton Trans.*, 2010, **39**, 4744.
- (a) A. Caneschi, D. Gatteschi, N. Lalioti, C. Sangregorio, R. Sessoli, G. Venturi, A. Vindigni, A. Rettori, M. G. Pini and M. A. Novak, *Angew. Chem., Int. Ed.*, 2001, **40**, 1760; (b) L. Bogani, A. Caneschi, M. Fedi, D. Gatteschi, M. Massi, M. A. Novak, M. G. Pini, A. Rettori, R. Sessoli and A. Vindigni, *Phys. Rev. Lett.*, 2004, **92**, 207204.
- T.-F. Liu, D. Fu, S. Gao, Y.-Z. Zhang, H.-L. Sun, G. Su and Y.-J. Liu, *J. Am. Chem. Soc.*, 2003, **125**, 13976.
- (a) Z.-M. Sun, A. V. Prosvirin, H.-H. Zhao, J.-G. Mao and K. R. Dunbar, *J. Appl. Phys.*, 2005, **97**, 10B305; (b) A. V. Palii, O. S. Reu, S. M. Ostrovsky, S. I. Klokishner, B. S. Tsukerblat, Z.-M. Sun, J.-G. Mao, A. V. Prosvirin, H.-H. Zhao and K. R. Dunbar, *J. Am. Chem. Soc.*, 2008, **130**, 14729.
- (a) L. Bogani, C. Sangregorio, R. Sessoli and D. Gatteschi, *Angew. Chem., Int. Ed.*, 2005, **44**, 5817; (b) L. Bogani, R. Sessoli, M. G. Pini, A. Rettori, M. A. Novak, P. Rosa, M. Massi, M. E. Fedi, L. Giuntini, A. Caneschi and D. Gatteschi, *Phys. Rev. B: Condens. Matter*, 2005, **72**, 064406.
- (a) T. Kajiwarra, M. Nakano, Y. Kaneko, S. Takaishi, T. Ito, M. Yamashita, A. Igashira-Kamiyama, H. Nojiri, Y. Ono and N. Kojima, *J. Am. Chem. Soc.*, 2005, **127**, 10150; (b) S. W. Przybylak, F. Tuna, S. J. Teat and R. E. P. Winpenny, *Chem. Commun.*, 2008, 1983.
- Y.-Z. Zheng, Z. Zheng and X.-M. Chen, *Coord. Chem. Rev.*, 2014, **258–259**, 1–15.
- Y.-Z. Zheng, M.-L. Tong, W.-X. Zhang and X.-M. Chen, *Angew. Chem., Int. Ed.*, 2006, **45**, 6310.
- Y.-Z. Zheng, W. Xue, M.-L. Tong, X.-M. Chen and S.-L. Zheng, *Inorg. Chem.*, 2008, **47**, 11202.

- 20 Y.-Z. Zheng, M.-L. Tong, W. Xue, W.-X. Zhang, X.-M. Chen, F. Grandjean, G. J. Long, S.-W. Ng, P. Panissoid and M. Drillon, *Inorg. Chem.*, 2009, **48**, 2028.
- 21 X.-N. Cheng, W.-X. Zhang, Y.-Z. Zheng and X.-M. Chen, *Chem. Commun.*, 2006, 3603.
- 22 Y.-Z. Zheng, M.-L. Tong, W. Xue, W.-X. Zhang, X.-M. Chen, F. Grandjean and G. J. Long, *Inorg. Chem.*, 2008, **47**, 4077.
- 23 S. Hu, L. Yun, Y.-Z. Zheng, Y. Lan, A. K. Powell and M.-L. Tong, *Dalton Trans.*, 2009, 1897.
- 24 H. Miyasaka and M. Yamashita, *Dalton Trans.*, 2007, 399.
- 25 (a) Y.-Z. Zheng, M. Speldrich, H. Schilder, X.-M. Chen and P. Kögerler, *Dalton Trans.*, 2010, **39**, 10827; (b) Y.-Z. Zheng and X.-M. Chen, *Dalton Trans.*, 2012, **41**, 11989; (c) Y.-Z. Zheng, L. Qin, Z. Zheng and X.-M. Chen, *Dalton Trans.*, 2013, **42**, 1770.
- 26 X.-N. Sui, X.-M. Lu, J.-H. Feng, S. Wang and P.-Z. Li, *J. Coord. Chem.*, 2008, **61**, 1568.
- 27 Y.-Z. Zheng, M. Speldrich, H. Schilder, X.-M. Chen and P. Kögerler, *CrystEngComm*, 2010, **12**, 1057.
- 28 W. Wernsdorfer, N. Aliaga-Alcalde, D. N. Hendrickson and G. Christou, *Nature*, 2002, **416**, 406.
- 29 R. L. Carlin, *Magnetochemistry*, Springer-Verlag, Germany, 1986.
- 30 O. Kahn, *Molecular Magnetism*, VCH, New York, 1993.
- 31 M. E. Fisher, *Am. J. Phys.*, 1964, **32**, 343.
- 32 U. Bossek, D. Nühlen, E. Bill, T. Glaser, C. Krebs, T. Weyhermüller, K. Wieghardt, M. Lengen and A. X. Trautwein, *Inorg. Chem.*, 1997, **36**, 2834.
- 33 (a) A. Fu, X. Huang, J. Li, T. Yuen and C. L. Lin, *Chem. – Eur. J.*, 2002, **8**, 2239; (b) X.-Y. Wang, L. Wang, Z.-M. Wang, G. Su and S. Gao, *Chem. Mater.*, 2005, **17**, 6369; (c) E.-Q. Gao, Z.-M. Wang and C.-H. Yan, *Chem. Commun.*, 2003, 1748.
- 34 S. Chikazumi, *Physics of Ferromagnetism*, Clarendon Press: Oxford Science Publications, Oxford, 1997, p. 521.
- 35 (a) P. M. Richards, *Phys. Rev. B: Solid State*, 1974, **10**, 4687; (b) P. Panissod and M. Drillon, in *Magnetism: Molecules to Materials*, ed. J. S. Miller and M. Drillon, Wiley-VCH Verlag, Berlin, 2001, vol. IV, pp. 234–270; (c) J. Souletie, P. Rabu and M. Drillon, in *Magnetism: Molecules to Materials*, ed. J. S. Miller and M. Drillon, Wiley-VCH Verlag, Berlin, 2005, vol. V, pp. 347–377.
- 36 (a) K. Sengupta, S. Rayaprol, K. K. Iyer and E. V. Sampathkumaran, *Phys. Rev. B: Condens. Matter*, 2003, **68**, 012411; (b) T. Suzuki, H. Nagai, M. Nohara and H. Takagi, *J. Phys.: Condens. Matter*, 2007, **19**, 145265.
- 37 (a) C. Coulon, R. Clérac, W. Wernsdorfer, T. Colin and H. Miyasaka, *Phys. Rev. Lett.*, 2009, **102**, 167204; (b) H. Miyasaka, K. Takayama, A. Saitoh, S. Furukawa, M. Yamashita and R. Clérac, *Chem. – Eur. J.*, 2010, **16**, 3656.
- 38 R. Sibille, T. Mazet, B. Malaman, T. Gaudisson and M. François, *Inorg. Chem.*, 2012, **51**, 2885.
- 39 (a) N. Ishii, Y. Okamura, S. Chiba, T. Nogami and T. Ishida, *J. Am. Chem. Soc.*, 2008, **130**, 24; (b) T. Ishida, Y. Okamura and I. Watanabe, *Inorg. Chem.*, 2009, **48**, 7012.
- 40 R. Sessoli, *Angew. Chem., Int. Ed.*, 2008, **47**, 5508.
- 41 J. Mydosh, *Spin Glasses: An Experimental Introduction*, Taylor & Francis, London, 1993.
- 42 Z. Fu, Y.-Z. Zheng, Y. Xiao, S. Bedanta, A. Senyshyn, G. G. Simeoni, Y. Su, U. Rücker, P. Kögerler and T. Brückel, *Phys. Rev. B: Condens. Matter*, 2013, **87**, 214406.
- 43 C. Coulon, R. Clérac, L. Lecren, W. Wernsdorfer and H. Miyasaka, *Phys. Rev. B: Condens. Matter*, 2004, **69**, 132408.
- 44 I. H. Schilder and H. Lueken, *J. Magn. Magn. Mater.*, 2004, **281**, 17.
- 45 I. L. Malaestean, M. Speldrich, S. G. Baca, A. Ellern, H. Schilder and P. Kögerler, *Eur. J. Inorg. Chem.*, 2009, 1011.
- 46 A. B. P. Lever, *Inorganic Electronic Spectroscopy*, Elsevier, Amsterdam, 1984, pp. 317–333.
- 47 B. N. Figgis and M. A. Hitchman, *Ligand Field Theory and Its Applications*, Wiley-VCH, New York, 2000.
- 48 (a) M. Evangelisti, F. Luis, L. J. de Jongh and M. Affronte, *J. Mater. Chem.*, 2006, **16**, 2534; (b) M. Evangelisti and E. K. Brechin, *Dalton Trans.*, 2010, **39**, 4672.